Lawrence Berkeley National Laboratory
LBL Publications

Title
Gamow–Teller transitions and neutron–proton-pair transfer reactions

Permalink
https://escholarship.org/uc/item/9qs68824

Authors
Van Isacker, P
Macchiavelli, AO

Publication Date
2018-05-01

DOI
10.1016/j.physletb.2018.03.034

Peer reviewed

Gamow–Teller transitions and neutron–proton-pair transfer reactions

P. Van Isacker [a,*], A.O. Macchiavelli [b]

[a] *Grand Accélérateur National d'Ions Lourds, CEA/DRF-CNRS/IN2P3, Bvd Henri Becquerel, F-14076 Caen, France*
[b] *Nuclear Science Division, Lawrence Berkeley National Laboratory Berkeley, CA 94720, USA*

A R T I C L E   I N F O

A B S T R A C T

We propose a schematic model of nucleons moving in spin–orbit partner levels, $j = l \pm \frac{1}{2}$, to explain Gamow–Teller and two-nucleon transfer data in $N = Z$ nuclei above ^{40}Ca. Use of the LS coupling scheme provides a more transparent approach to interpret the structure and reaction data. We apply the model to the analysis of charge-exchange, ^{42}Ca(^{3}He,t)^{42}Sc, and np-transfer, ^{40}Ca(^{3}He,p)^{42}Sc, reactions data to define the elementary modes of excitation in terms of both isovector and isoscalar pairs, whose properties can be determined by adjusting the parameters of the model (spin–orbit splitting, isovector pairing strength and quadrupole matrix element) to the available data. The overall agreement with experiment suggests that the approach captures the main physics ingredients and provides the basis for a boson approximation that can be extended to heavier nuclei. Our analysis also reveals that the SU(4)-symmetry limit is not realized in ^{42}Sc.

In two recent papers Fujita et al. [1,2] report on results of (^{3}He,t) charge-exchange experiments that determine Gamow–Teller (GT) strength in nuclei with mass numbers $A = 42, 46, 50$ and 54. They observe a concentration of most of the GT strength in the lowest 1^+ state at 0.611 MeV in the ^{42}Ca $\rightarrow$ ^{42}Sc reaction and, as A increases, a migration of this strength to higher energies. Both features can be reproduced either by a shell-model calculation with a realistic interaction in the pf shell or by calculations in the quasi-particle random phase approximation that include an isoscalar (or spin-triplet) interaction. The migration of the strength towards higher energies with A can be understood intuitively as a result of the increasing importance of the $\nu 0f_{7/2} \rightarrow \pi 0f_{5/2}$ component of the GT transition. The low-energy strength in ^{42}Sc is more difficult to fathom and is attributed to the isoscalar component of the residual nuclear interaction. As a result, the authors [1,2] claim the 1_1^+ level in ^{42}Sc to be a "low-energy super GT state", and its existence is attributed to the restoration of Wigner's SU(4) symmetry [3].

Relevant to these studies are the results of earlier measurements of two-nucleon transfer using the ^{40}Ca(^{3}He,p)^{42}Sc reaction [4,5]. The coherent properties of the transfer mechanism of the neutron–proton (np) pair, in both isospins channels, provide a complementary tool to probe the wave functions of the low-lying 0^+ and 1^+ levels in ^{42}Sc. The comparable cross-sections to

these states appear, *a priori*, at odds with the "super GT" conjecture above.

In this letter we propose an explanation of these observations, assuming that the nucleons occupy two orbitals with radial quantum number n, orbital angular momentum l and total angular momentum $j = l \pm \frac{1}{2}$. This is the analogue of a single-j approximation, for example the $0f_{7/2}$ model [6], but for an l orbital. Since the properties of the nuclear interaction are more transparent in LS coupling, we analyze the problem in this basis instead of the more usual jj coupling. Results are of course independent of the chosen basis and generally intermediate between the two bases [7]. Two nucleons with isospin projection $T_z = \pm 1$, angular momentum $J = 0$ and isospin $T = 1$ have two possible components with $(LS) = (00)$ and (11), where L refers to the orbital angular momentum of the two nucleons and S to their spin. Three states with $(JT) = (10)$ occur for a neutron–proton pair and they are admixtures of $(LS) = (01), (10)$ and (21). One state with $(JT) = (11)$ exists for $T_z = 0$ and it has $(LS) = (11)$. These are the only states that enter into the discussion of the GT strength and np transfer.

The character of the eigenstates of a nuclear Hamiltonian in this basis is first of all determined by the one-body spin–orbit term

$$\hat{H}_{\text{so}} = \epsilon_- \hat{n}_- + \epsilon_+ \hat{n}_+ = \Delta\epsilon \, \tfrac{1}{2}(\hat{n}_- - \hat{n}_+) + \bar{\epsilon}\,\hat{n}, \qquad (1)$$

where $\hat{n}$ is the nucleon-number operator, $\hat{n}_\pm$ are the nucleon-number operators for the two orbitals $j = l \pm \frac{1}{2}$ with single-particle energies $\epsilon_\pm$, $\Delta\epsilon \equiv \epsilon_- - \epsilon_+$ and $\bar{\epsilon} \equiv \frac{1}{2}(\epsilon_- + \epsilon_+)$. The operator $\hat{H}_{\text{so}}$

*   Corresponding author.
    E-mail address: isacker@ganil.fr (P. Van Isacker).

is a non-diagonal one-body operator in the $(LSJT)$ basis with the following matrices:

- for $(JT) = (01)$ in the basis $(LSJT) = (0001)$ and (1101):

$$2\bar{\epsilon} + \frac{\Delta\epsilon}{2l+1} \begin{bmatrix} -1 & \sqrt{4l(l+1)} \\ \sqrt{4l(l+1)} & 1 \end{bmatrix}; \qquad (2)$$

- for $(JT) = (11)$ in the basis $(LSJT) = (1111)$:

$$2\bar{\epsilon}; \qquad (3)$$

- for $(JT) = (10)$ in the basis $(LSJT) = (0110)$, (1010) and (2110):

$$2\bar{\epsilon} + \frac{\Delta\epsilon}{2l+1} \begin{bmatrix} -1 & -\sqrt{\frac{4l(l+1)}{3}} & 0 \\ -\sqrt{\frac{4l(l+1)}{3}} & -1 & \sqrt{\frac{2(2l-1)(2l+3)}{3}} \\ 0 & \sqrt{\frac{2(2l-1)(2l+3)}{3}} & 2 \end{bmatrix}. \qquad (4)$$

For each (JT) a complete set $(LSJT)$ is given and therefore the diagonalization of the above matrices leads to the correct eigenvalues $2\epsilon_-$, $\epsilon_- + \epsilon_+$ and/or $2\epsilon_+$. Matrices for different (JT) can be constructed likewise but the ones given in Eqs. (2) to (4) suffice for the applications considered below.

To $\hat{H}_{so}$ must be added contributions from the two-body interaction $\hat{V}$, which can have diagonal matrix elements $V_{LSJT} \equiv \langle LSJT|\hat{V}|LSJT \rangle$ as well as off-diagonal ones $\langle LSJT|\hat{V}|L'S'JT \rangle$, where it is assumed that the interaction is invariant under rotations in physical and isospin space and therefore conserves J and T.

The structure of the eigenstates is mostly determined by the splitting $\Delta\epsilon$, to which the interactions V_{LSJT} provide a correction. Off-diagonal matrix elements due to spin-dependent or tensor forces are small compared to those induced by $\hat{H}_{so}$ and can be neglected in this context, $\langle LSJT|\hat{V}|L'S'JT \rangle \approx 0$ if $(LS) \neq (L'S')$. Furthermore, the nuclear interaction in spatially anti-symmetric states (L odd) is weak, $V_{11J1} \approx V_{1010} \approx 0$. These approximations follow from the short-range attractive nature of the residual nuclear interaction and are exactly satisfied by a delta interaction [8]. They lead to a description of structural properties in terms of three essential quantities: the spin–orbit splitting $\Delta\epsilon$, and the isoscalar and isovector pairing strengths V_{0110} and V_{0001}, which we denote from now on as g_0 and g_1, respectively. There is an additional dependence on the quadrupole matrix element V_{2110}, which appears in the $(JT) = (10)$ matrix, but this dependence is weak and the value of V_{2110} can be estimated from data (see below).

To calculate various properties in the $LSJT$ basis, we consider a general one-body operator with definite tensor character λ_l under $SO_L(3)$, λ_s under $SO_S(3)$, coupled to total λ_j, and λ_t under $SO_T(3)$. It has the matrix elements

$$\langle l^2 LSJT|||\sum_i [\hat{t}_i^{(\lambda_l)} \times \hat{t}_i^{(\lambda_s)}]^{(\lambda_j)} \hat{t}_i^{(\lambda_t)}|||l^2 L'S'J'T' \rangle$$

$$= -2[\lambda_j][L][S][J][T][L'][S'][J'][T']\langle l\|\hat{t}^{(\lambda_l)}\|l\rangle \langle \tfrac{1}{2}\|\hat{t}^{(\lambda_s)}\|\tfrac{1}{2}\rangle$$

$$\times \langle \tfrac{1}{2}\|\hat{t}^{(\lambda_t)}\|\tfrac{1}{2}\rangle (-)^{\lambda_l + \lambda_s + \lambda_t} \begin{Bmatrix} L & S & J \\ L' & S' & J' \\ \lambda_l & \lambda_s & \lambda_j \end{Bmatrix} \begin{Bmatrix} L & L' & \lambda_l \\ l & l & l \end{Bmatrix}$$

$$\times \begin{Bmatrix} S & S' & \lambda_s \\ \tfrac{1}{2} & \tfrac{1}{2} & \tfrac{1}{2} \end{Bmatrix} \begin{Bmatrix} T & T' & \lambda_t \\ \tfrac{1}{2} & \tfrac{1}{2} & \tfrac{1}{2} \end{Bmatrix}, \qquad (5)$$

where the symbols in curly brackets are $6j$- and $9j$-coefficients [8] and with $[x] \equiv \sqrt{2x+1}$. The triple bars on the left-hand side indicate that the matrix element is reduced in J and T, while the double-barred matrix elements on the right-hand side are singly reduced in L, S or T. With this expression one can calculate matrix elements of the M1 operator ($\lambda_j = 1$), which has spin ($\lambda_l, \lambda_s) = (0,1)$, orbital ($\lambda_l, \lambda_s) = (1,0)$ and tensor ($\lambda_l, \lambda_s) = (1,1)$ parts of both isoscalar ($\lambda_t = 0$) and isovector ($\lambda_t = 1$) character. For the GT operator one takes ($\lambda_l, \lambda_s, \lambda_j, \lambda_t) = (0,1,1,1)$. One finds three allowed GT transitions, namely $(LS) = (00) \to (01)$, $(11) \to (10)$ and $(11) \to (11)$. The strengths are independent of the orbital angular momentum l with JT-reduced matrix elements given by $-\sqrt{18}$, $\sqrt{6}$ and $-\sqrt{24}$, respectively.

To obtain predictions for the np-transfer strengths, we treat the ground state of ^{40}Ca as the vacuum $|o\rangle$ and write the wave functions of the 0_i^+ and 1_i^+ states in ^{42}Sc as

$$|^{42}\text{Sc}(0_i^+)\rangle = \alpha_{00}^i |l^2 0001\rangle + \alpha_{11}^i |l^2 1101\rangle,$$
$$|^{42}\text{Sc}(1_i^+)\rangle = \alpha_{01}^i |l^2 0110\rangle + \alpha_{10}^i |l^2 1010\rangle + \alpha_{21}^i |l^2 2110\rangle, \qquad (6)$$

with coefficients α_{LS}^i obtained from the diagonalization of the matrices (2) and (4). In LS coupling the $L = 0$ transfer strengths follow naturally from

$$|\langle ^{42}\text{Sc}(0_i^+)\|A_{L=0,S=J=0,T=1}^\dagger\|^{40}\text{Ca}(0_1^+)\rangle|^2 = (\alpha_{00}^i)^2,$$
$$|\langle ^{42}\text{Sc}(1_i^+)\|A_{L=0,S=J=1,T=0}^\dagger\|^{40}\text{Ca}(0_1^+)\rangle|^2 = 3(\alpha_{01}^i)^2, \qquad (7)$$

where $A_{LSJT}^\dagger$ is a two-nucleon creation operator.

We apply the above schematic model to the properties of $A = 42$ nuclei. We fix the spin–orbit splitting to its value taken in Refs. [1,2], $\Delta\epsilon = 6$ MeV, and vary the pairing strengths g_0 and g_1. We take as a first estimate equal isoscalar and isovector pairing strengths, and allow for a variation of 15% of the isoscalar strength, that is, we consider $g_0 = g_1/x$ with x between 0.85 and 1.15, indicated by shaded bands around the 'canonical' estimate $g_0 = g_1$. In this way the sensitivity of the various properties to the ratio of isoscalar-to-isovector pairing strengths is highlighted. The quadrupole matrix element $V_{2110} \approx V_{2021}$ is fixed such that the excitation energy of the 2_1^+ level in ^{42}Ca (1.525 MeV) is reproduced. Essentially the same results are obtained if V_{2110} is varied within a wide range.

Results are summarized in Fig. 1. Panel (a) shows the excitation energies of levels in ^{42}Sc (relative to the 0^+ level) as a function of the pairing strengths. The 1_1^+ level is at an essentially constant energy for $g_0 = g_1$ but its energy is very sensitive to the ratio of the two pairing strengths. The near-degeneracy of the $(JT) = (01)$ and (10) states, therefore, cannot be used as an indication of Wigner's SU(4) symmetry in ^{42}Sc, which is only realized in the extreme limit of $g_0 = g_1 \gg \Delta\epsilon$. On the other hand, it is to be expected that the isovector pairing strength g_1 can be constrained from the corresponding observed pairing gap. The "pairing gap" for the odd-mass nucleus ^{41}Ca, that is, the binding-energy difference

$$\Delta^{(3)} = \frac{1}{2}\left[\text{BE}(^{42}\text{Ca}) + \text{BE}(^{40}\text{Ca}) - 2\text{BE}(^{41}\text{Ca})\right], \qquad (8)$$

is the only quantity of this kind that is available within our schematic model. Its experimental value of 1.5585 MeV is also shown in panel (a) of Fig. 1 and fixes the isovector pairing strength to $g_1 \approx -5$ MeV.

Panel (b) shows the $B(\text{M1}; 1_i^+ \to 0_1^+)$ values in ^{42}Sc, calculated with a spin quenching factor of 0.74. The M1 strength from the 1_1^+ level is known experimentally [9], $B(\text{M1}; 1_1^+ \to 0_1^+) = 6.1(2.7) \ \mu_N^2$, but its error is too large to constrain the pairing strength.
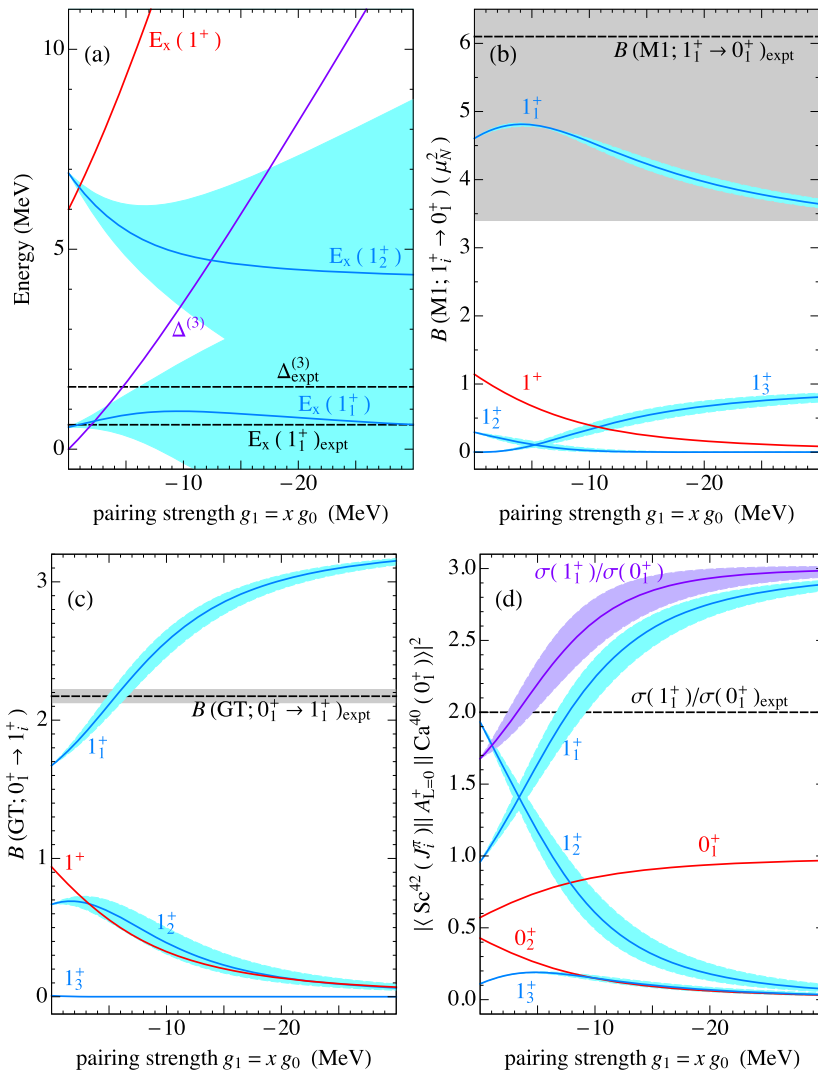
Fig. 1. (Color online.) Results for (a) excitation energies in ^{42}Sc and the pairing gap $\Delta^{(3)}$, (b) $B(M1; 1_1^+ \to 0_1^+)$ values in ^{42}Sc, (c) $B(GT; 0_1^+ \to 1_i^+)$ strength in the ^{42}Ca $\to$ ^{42}Sc reaction and (d) cross-sections for the ^{40}Ca $\to$ ^{42}Sc reaction. Experimental values are indicated by the black dashed lines with uncertainties in gray. The results of the schematic model are in blue for $T = 0$ and in red for $T = 1$ states. The calculated pairing gap $\Delta^{(3)}$ in panel (a) and the calculated ratio of cross-sections $\sigma(1_1^+)/\sigma(0_1^+)$ in panel (d) are in purple. All curves are for equal isoscalar and isovector strengths $g_0 = g_1$, and the shaded areas around them are obtained for $g_0 = g_1/x$ with x varying between 0.85 and 1.15.

Panel (c) shows the $B(GT; 0_1^+ \to 1_i^+)$ strength for the ^{42}Ca(^{3}He,t)^{42}Sc charge-exchange reaction, using the same quenching factor as in the spin part of the M1 operator. Experimentally, most of the observed strength is concentrated in the 1^+ state at 0.611 MeV [1,2], which is indicated in the figure, with some fragmentation at higher energies (not shown). This is in qualitative agreement with the schematic model, where the main strength is indeed found in the 1_1^+ level with some minor components in two excited 1^+ states with $T = 0$ and $T = 1$, respectively. Note also that the uncertainty associated with the ratio of pairing strengths is fairly small for the GT strength.

Finally, panel (d) shows results for the ^{40}Ca $\to$ ^{42}Sc np-transfer reaction. We pay particular attention to the ratio of squared amplitudes from Eq. (7) that gives directly the ratio of cross-sections, $\sigma(1_1^+)/\sigma(0_1^+)$. The experimental ratio, $\sim$2, is consistent with our results at the value of the pairing strength g_1, derived from the $B(GT)$ measurement and from the pairing gap $\Delta^{(3)}$. A better agreement would be expected by introducing small admixtures of the $p_{3/2}$ and $p_{1/2}$ orbits, not included in the schematic model. We note here that we have also checked the calculated ratio in the

jj-coupling scheme by transforming the pair amplitudes into their corresponding $f_{7/2}^2$, $f_{5/2}^2$ and $f_{7/2}f_{5/2}$ (for $T = 0$) components, which were used in DWUCK4 [10] to calculate the cross-sections at forward angles ($L = 0$ transfer).

The available experimental data [2,5,9] are summarized in Table 1 and compared with the results of the schematic model. The latter are obtained with spin–orbit splitting $\Delta\epsilon = 6$ MeV and pairing strengths $g_0 = g_1 = -5$ MeV. The isoscalar pairing strength g_0 is varied by 15% around g_1 to obtain an estimate of the theoretical uncertainty. Because of the restricted model space with only the f orbital, several observed levels are absent from the theory, as indicated with a dashed line.

We can now also study the components in LS coupling of the yrast 0^+ and 1^+ states, for which the schematic model should be reliable. Table 2 lists the amplitudes of 0_1^+ and 1_1^+, written in the $(LSJT)$ basis of Eqs. (2) and (4). It is seen that the spatially unfavored components (L odd) are important, which contradicts the assumption of SU(4) symmetry. The fact that nevertheless a strong $B(GT; 0_1^+ \to 1_1^+)$ is observed is due to the constructive addition of the $L = 0 \to L = 0$ and $L = 1 \to L = 1$ transitions. Also shown in

Table 1

Summary of available experimental data [2,5,9] and the results of the schematic model for the adopted values of the parameters.

Probe	^{42}Sc level		Experiment	Schematic model[a]
	J^π	E_x (MeV)		
(^{3}He,p)			Relative Intensity	
	0_1^+	0	1	1
	1_1^+	0.61	2	2.20(17)
	$(0^+, 1^+)$	1.89	0.17	–
	1^+	3.69	1.3	1.57(16)
	1^+	3.86	0.38	–
(^{3}He,t)			B(GT)	
	1_1^+	0.61	2.17(5)	2.11(8)
	1^+	1.89	0.097(3)	–
	1^+	3.69	0.127(3)	0.62(8)
Lifetime			B(M1) (μ_N^2)	
DSAM	1_1^+	0.61	6.1(2.7)	4.80(2)

[a] The theoretical uncertainties correspond to a $\pm 15\%$ variation in the isoscalar pairing strength g_0, as discussed in the text.

Table 2

LS-coupling amplitudes (in %) of the yrast 0^+ and 1^+ states of ^{42}Sc, in the schematic model and for the KB3G interaction.

	Schematic model			KB3G (f^2)		
	$L=0$	$L=1$	$L=2$	$L=0$	$L=1$	$L=2$
0_1^+	75	25	–	73	23	–
1_1^+	55	31	14	65	26	4

Table 2 are the corresponding components for the modified Kuo–Brown KB3G Hamiltonian [11], which is a realistic interaction for the entire pf shell [12]. The f^2 components carry the majority of the strength ($\sim 95\%$) and the mixing of spatially favored and unfavored components is consistent with that found in the schematic model.

In summary, charge-exchange and np-transfer reactions define the elementary modes with isovector and isoscalar pairs that are spatially favored as well as unfavored. We have applied this approach to ^{40,42}Ca $\rightarrow$ ^{42}Sc reactions to determine the nature of these elementary modes. Good agreement with the experimental data suggests the adequacy of the model. Although the 1_1^+ state carries a large fraction of the GT strength, our analysis of both (^{3}He,t) and (^{3}He,p) reactions points out that the SU(4)-symmetry limit is not reached, as the spin–orbit potential breaks the LS-coupling scheme. The elementary pairs thus determined can be treated as bosons, leading to an interpretation of GT and np-transfer data in heavier $0f_{7/2}$ nuclei in terms of an interacting boson model—an approach which is currently under study. We believe that this may provide an intuitive and simple picture, which is complementary to state-of-the-art shell-model calculations.

Acknowledgements

References

[1] Y. Fujita, et al., Phys. Rev. Lett. 112 (2014) 112502.
[2] Y. Fujita, et al., Phys. Rev. C 91 (2015) 064316.
[3] E.P. Wigner, Phys. Rev. 51 (1937) 106.
[4] R.W. Zurmühle, C.M. Fou, L.W. Swenson, Nucl. Phys. 80 (1966) 259.
[5] F. Pühlhofer, Nucl. Phys. 116 (1968) 516.
[6] J.D. McCullen, B.F. Bayman, L. Zamick, Phys. Rev. 134 (1964) B515.
[7] N. Zeldes, Phys. Rev. 90 (1953) 416.
[8] I. Talmi, Simple Models of Complex Nuclei. The Shell Model and the Interacting Boson Model, Harwood, Chur, 1993.
[9] Evaluated nuclear structure data file database, http://www.nndc.bnl.gov/ensdf/.
[10] P.D. Kunz, DWUCK4 Program Manual, University of Colorado, spot.colorado.edu/~kunz/DWBA.html.
[11] A. Poves, J. Sánchez-Solano, E. Caurier, F. Nowacki, Nucl. Phys. A 694 (2001) 157.
[12] E. Caurier, G. Martínez-Pinedo, F. Nowacki, A. Poves, A.P. Zuker, Rev. Mod. Phys. 77 (2005) 427.